Hindered Internal Rotations in Van der Waals Molecules and Molecular Crystals

W. J. BRIELS, J. TENNYSON, M. CLAESSENS, TH. VAN DER LEE, AND A. VAN DER AVOIRD

Institute of Theoretical chemistry, University of Nijmegen, Toernooiveld, Nijmegen, The Netherlands

Abstract

The quantum dynamical behavior of the Van der Waals molecule $(N_2)_2$ and that of the ordered α and γ phases of solid N_2 have recently been calculated, starting from the same *ab initio* N_2—N_2 potential. By interpreting the results of these calculations we try to improve our understanding of the libration/internal rotation motions of the N_2 monomers and the orientational order–disorder (α-β) phase transition. Some new results are presented and further (mean-field and libron-model) calculations are proposed which assess explicitly the intermolecular pair correlation effects caused by the anisotropic interaction potential.

1. Introduction

Van der Waals molecules, which are weakly bound complexes of normal molecules, can be considered as small segments of molecular crystals. The study of these complexes in conjunction with molecular crystals is very illustrative and useful. In the first place, their dynamical behaviour, although it lacks the collective aspects, shows many of the typical characteristics found in molecular solids. Here, we concentrate on orientational order–disorder transitions, i.e., the transitions from bending vibrations (librations) to more or less free internal rotations. Classical Monte Carlo calculations [1] on $(CO_2)_n$ clusters with $n = 2$ to 13 have shown that complexes as small as dimers ($n = 2$) exhibit remarkably sharp order–disorder phase transitions, as a function of temperature. Since Van der Waals molecules are considerably simpler than molecular crystals, their dynamical properties can be calculated in much more detail by both classical and quantum mechanical methods.

Second, Van der Waals molecules provide the most sensitive tests of intermolecular potentials, especially in the physically important region around the Van der Waals minimum [2]. Although it has also been advocated [3] that molecular crystals and, in particular, their phonon dispersion relations, are very useful in this respect, we note that the route from the intermolecular potential to the phonon frequencies that can be compared with experiment, involves approximations, such as the assumption of pairwise additivity for the potential and the (usually harmonic) model for the lattice dynamics. For simple Van der Waals molecules, on the other hand, accurate dynamical calculations can be performed which lead directly from a given potential to the rovibrational spectrum.

As an example we study nitrogen. Apart from extensive work [3,4] on solid N_2, which has two ordered (α and γ) phases and one orientationally disordered (β) phase, there is also much interest in gas and liquid properties [5-7]. An important part of

this work is concerned with extracting empirical N_2—N_2 interaction potentials [3] from the experimental data. Recently, a detailed N_2—N_2 potential has been obtained from *ab initio* calculations [8,9]. This potential has been successfully used in lattice dynamics studies [10] on α and γ N_2 and, at the same time, in accurate dynamical calculations [11] on the Van der Waals molecule $(N_2)_2$. In the present paper, we discuss some new results and ways to extract further useful information.

2. Lattice Dynamics of Solid N_2

Using the *ab initio* N_2—N_2 potential in its site–site representation [9] with the force centres shifted on the N—N axes, away from the nuclei, Luty et al. [10] have performed lattice dynamics calculations on the ordered cubic (α) and tetragonal (γ) N_2 crystal phases. They applied not only the usual harmonic method [12], but also the self-consistent phonon (SCP) method [12] which corrects for the anharmonicity of the potential by using effective force constants obtained by (quantum mechanical and thermal) averaging over the molecular displacements in the crystal. In the generalization of the SCP method from atomic (rare gas) crystals [13] to molecular solids [14] it had to be assumed, however, that the librations have small amplitudes.

The results [10] are generally in good agreement with experiment: lattice constants, cohesion energy, the phonon frequencies and their pressure or volume dependence (Grüneisen parameters). This is the more satisfactory since no adjustments of the ab initio potential to the crystal data have been made (in contrast with the usual semi-empirical treatments [3]). For the translational phonon modes the agreement is almost perfect: the frequencies are only 4% higher than the neutron scattering results (11% higher if one neglects anharmonicity). For the librational modes the agreement is somewhat less good: the frequencies are overestimated by 28% on the average (34% in the harmonic model). Also these modes do not soften sufficiently with increasing temperature. This is not surprising, however, as the librational displacements are actually not small even at low temperature (estimated [3] root-mean-square displacement 17 deg at $T = 20$ K). When the temperature rises to the α–β phase transition point, the N_2 rotations in the crystal become more and more free. So, one may expect that the generalized SCP method [14] breaks down for the librational modes.

A model which is better, in principle, at describing the librations in solid N_2 and their change into hindered rotations which occurs at the α–β phase transition is the so-called libron model [15–17]. In this model it is assumed that the angular vibrations of the molecules can be expanded in a basis of free-rotor functions. In case of linear molecules such as N_2 these are simply spherical harmonics $Y_{j,m}(\theta,\phi)$, where θ and ϕ are the angular displacement coordinates which can adopt any value in the range $0 \leq \theta < \pi, \quad 0 \leq \phi < 2\pi$. The lattice dynamics treatment starts with a mean-field calculation [17]; the wave functions emerging are then used in the "libron" model which accounts for the pair correlation effects caused by the anisotropic intermolecular potential, and, at the same time, introduces dispersion (dependence on the wave vector $\mathbf{q}$) into the libron frequencies.

For solid N_2 several of such libron model calculations have been made [15–17],

always using approximate empirical potentials. The most advanced one is that by Dunmore [16] who has summed the intermolecular potential over six shells (86 neighboring molecules) in the α-N_2 lattice, but has still neglected terms in the crystal potential which have nonazimuthal symmetry around the equilibrium N_2 axes (i.e., the ϕ dependence of the mean-field potential). In all these libron treatments it has been assumed that the translational vibrations of the molecules in the lattice are completely decoupled from the angular motions. Actually, in crystals which have inversion symmetry, such as N_2, the translations and the librations do separate at some points in the Brillouin zone (for the optical modes at $\mathbf{q} = 0$, for instance), but the translational displacements still influence the effective librational potential. This effect is neglected by keeping the molecules with their centres fixed at the lattice points.

Here, we present some new results obtained by utilizing the same *ab initio* N_2—N_2 potential [9] that was used previously in the harmonic and SCP lattice dynamics calculations [10]. Instead of the site–site representation, we have now employed the spherical expansion of this potential, however, which is more convenient in this case and which has also been used for the $(N_2)_2$ dimer [11] (see Sec. 3). The spherically expanded potential reads for a pair of molecules A and B:

$$V_{AB} = (4\pi)^{3/2} \sum_{L_A,L_B,L} v_{L_A,L_B,L}(R) A_{L_A,L_B,L}(\theta_A,\phi_A,\theta_B,\phi_B,\Theta,\Phi), \tag{1}$$

where the angular functions are defined as

$$A_{L_A,L_B,L} = \sum_{M_A,M_B,M} \begin{pmatrix} L_A & L_B & L \\ M_A & M_B & M \end{pmatrix} Y_{L_A,M_A}(\theta_A,\phi_A) Y_{L_B,M_B}(\theta_B,\theta_B) Y(\Theta,\Phi), \tag{2}$$

with R being the distance between the centres of A and B, θ_A,ϕ_A and θ_B,ϕ_B describing the orientations of the molecular axes and Θ and Φ the orientation of the vector $\mathbf{R}$, relative to some lattice coordinate system. The expression in brackets is a 3-j symbol [18]. The *ab initio* calculations [8,9] have demonstrated that anisotropic terms in potential (1) up to $L_A = L_B = 4$ inclusive are important; actually some higher terms were included as well [9].

Summing this potential over six shells (86 neighbouring molecules), just as Dunmore [16], but making no further approximations, mean-field calculations have been carried out [19] for α-N_2 in the cubic Pa3 structure [4]. The spherical harmonic basis was extended to $j = 10$ (66 functions) for *ortho*-N_2 and to $j = 9$ (55 functions) for *para*-N_2. The results listed in Table I demonstrate that this is sufficient to converge the ground state cohesion energy to within 0.5 cm^{-1} and the first excitation energy to within 1 cm^{-1}; the mean-field iterations were always convergent in three cycles.

The first excitation frequency 50 cm^{-1} is very close to the value of 51 cm^{-1} calculated by Dunmore [16], which is surprising as our anisotropic *ab initio* N_2—N_2 potential [9] is rather different from the empirical potential used by Dunmore [16], see Table II. The difference between *ortho*-N_2 and *para*-N_2 crystals is small. Actually, it would be interesting if this difference could be observed since it presents a measure for the degree of orientational rigidity of the N_2 crystal phases (γ, α, and β). In the completely rigid case, the *ortho*- and *para*-N_2 results would be identical [16]; if the N_2 molecules are free internal rotors, such as H_2 molecules in the solid, the excitation

TABLE I.   Mean-field results for the α-N_2 crystal (lattice constant a = 5.644 Å) using
the *ab initio* N_2—N_2^* potential [9]. Total librational energy E_0 and first excitation
frequency ω as functions of the spherical harmonic basis size for *ortho*- and *para*-N_2.

ortho			para		
j_{max}(size)	E_0(kJ/mol)*	ω(cm^{-1})	j_{max}(size)	E_0(kJ/mol)*	ω(cm^{-1})
2 (6)	-6.253	128.7	3(10)	-6.551	100.5
4(15)	-6.711	79.0	5(21)	-6.791	65.3
6(28)	-6.829	57.3	7(36)	-6.844	53.0
8(45)	-6.849	51.2	9(55)	-6.850	50.4
10(66)	-6.851	50.2			

* Includes the librational zero-point energy (well depth E_e = 7.436 kJ/mol), but not the
zero-point energy corresponding with the translational lattice vibrations. Experimental
cohesion energy 6.92 kJ/mol.

frequencies would differ by 8 cm^{-1}. Also in the $(N_2)_2$ dimer there is a noticeable
difference between *ortho–ortho*, *ortho–para*, and *para–para* complexes [11].

It is striking that the mean-field spectrum is very similar to that of a two-dimensional
harmonic oscillator, just as Dunmore [16] has found with his empirical potential. This
justifies the application of his libron model, in order to take the pair correlation effects
into account. It appeared [16] that, for $q = 0$, this gives a significant lowering of the
mean-field librational frequencies bringing them into good agreement with the ex-
perimental values. We intend to proceed with this model and, also, we will attempt
to include the effects of the translational lattice vibrations by combining the libron
model with the self-consistent phonon model or by a renormalization procedure.

3. Dynamics of the Van der Waals Molecule ($N_2)_2$

The questions which are pertinent to the understanding of the librational motions
in solid N_2 and the α–β phase transition, what is the importance of pair correlation
effects and how well does the libron model account for these effects, can be answered
explicitly for the $(N_2)_2$ dimer. The dynamics of this dimer is also interesting by itself,
however, since the $(N_2)_2$ complex can be expected to lie between a normal molecule
with a near-rigid nuclear framework and a system in which the nuclear positions are
completely undefined. We are familiar with the latter situation for electrons in atoms
and molecules; for the nuclei it is rather unusual, but it occurs in noble gas–H_2 [2]
and $(H_2)_2$ [20,21] complexes where the H_2 molecules are practically free quantum
mechanical internal rotors.

The *ab initio* potential [9] favors a crossed equilibrium structure for the $(N_2)_2$ dimer
with D_e = 122 cm^{-1} and R_e = 3.5 Å. There are different barriers to internal rotations:
25 cm^{-1} through the parallel structure with R_m = 3.6 Å and 40 cm^{-1} through the
T-shaped structure with R_m = 4.2 Å. Using the spherical expansion (1) of this po-
tential (in a body-fixed frame with $\Theta = \Phi = 0$, $\phi = \phi_A - \phi_B$), accurate dynamical

TABLE II. Spherical expansion (1) of the *ab initio* N_2—N_2 potential [9], compared with the empirical potential of Raich and Mills used by Dunmore [16]. The expansion coefficients $v_{L_A,L_B,L}(R)$ are tabulated (in cm^{-1}) for the nearest ($R = 3.991$ Å) and next-nearest ($R = 5.644$ Å) neighbor distances in the α-N_2 lattice.

			R = 3.991 Å		R = 5.644 Å	
L_A	L_B	L	empirical [16]	ab initio [9]	empirical [16]	ab initio [9]
0	0	0	-79.351	-55.345	-17.834	-13.831
2	0	2	15.905	32.359	- 1.311	- 1.011
2	2	0	3.104	5.564	- 0.053	- 0.015
2	2	2	- 6.144	- 9.146	- 0.112	- 0.002
2	2	4	25.628	39.239	2.833	2.555
4	0	4	5.513	8.635	0.035	0.007
4	2	2	0.820	0.629	0.001	
4	2	4	- 1.160	- 1.467	- 0.002	- 0.001
4	2	6	2.816	10.282	0.010	0.356
4	4	0	0.087	0.010		
4	4	2	- 0.114	- 0.012		
4	4	4	0.165	0.052		
4	4	6	- 0.307	- 0.263		
4	4	8	0.875	4.052	0.001	0.089
6	0	6	0.816	0.779	0.002	0.001
6	2	4	0.132	0.022	0.001	
6	2	6	- 0.200	- 0.114		
6	2	8	0.533	1.075		0.013

calculations have just been finished [11]. These start from the exact (rigid monomer) ro-vibrational Hamiltonian including centrifugal distortions and Coriolis interactions [22]

$$H = - \frac{\hbar^2}{2\mu R} \frac{\partial^2}{\partial R^2} R + \frac{|\mathbf{J} - \mathbf{j}|^2}{2\mu R^2} + \frac{j_A^2}{2\mu_A r_A^2} + \frac{j_B^2}{2\mu_B r_B^2} + V_{AB}(R, \theta_A, \theta_B, \phi), \qquad (3)$$

where $\mathbf{j}_A$ and $\mathbf{j}_B$ are the monomer angular momenta associated with the body fixed angles (θ_A, ϕ_A) and (θ_B, ϕ_B), respectively, $\mathbf{j} = \mathbf{j}_A + \mathbf{j}_B$; $\mathbf{J}$ describes the overall rotation; μ, μ_A, and μ_B are the dimer and monomer reduced masses; and r_A and r_B are the (fixed) N_2 monomer bond lengths. An appropriate and convenient basis to calculate the bound states of Hamiltonian (3) is the following:

$$\chi_n(R) \, \mathcal{Y}_{j_A, j_B}^{j,k}(\theta_A, \phi_A, \theta_B, \phi_B) D_{M,k}^J(\alpha, \beta, 0), \qquad (4)$$

with $D^J_{M,k}$ being overall rotation functions. The generalized spherical harmonics are defined as

$$\mathcal{Y}^{j,k}_{j_A,j_B} = \sum_{m_A,m_B} Y_{j_A,m_A}(\theta_A,\phi_A)Y_{j_B,m_B}(\theta_B,\phi_B)(j_A,m_A;j_B,m_B|j,k), \qquad (5)$$

and the radial (Morse oscillator) functions (in terms of normalized associated Laguerre functions L^α_n) as [23]

$$\chi_n(R) = \beta^{1/2}y^{(\alpha+1)/2}e^{-y/2}L^\alpha_n(y),$$

with

$$y = A \quad \exp[\beta(R - R_e)]. \qquad (6)$$

Using this basis the secular problem over the full Hamiltonian (3) has been solved, after symmetry adaptation to the permutation-inversion group $S'_4 \otimes C_i$ [11]. The parameters β and A (and hence α, which is the integer closest to A) are related to those of the Morse potential for diatomic molecules [24]

$$A = 4D_e/\omega_e, \quad \beta = \omega_e(\mu/2D_e)^{1/2}.$$

In the $(N_2)_2$ dynamical calculation [11], the Morse parameters R_e, D_e, and ω_e were variationally optimized.

Basis (4) consists of free rotor functions [spherical harmonics, Eq. (5), which are coupled for computational convenience] in the internal angular coordinates. However, in the ground state, the A^+_1 state for the $ortho$-N_2–$ortho$-N_2 complex and the B^-_2 state for the $para$–$para$ complex, the monomers are rather well localized around the equilibrium configuration, see Figure 1. Actually, there are two equivalent equilibrium configurations with $\phi = 90°$ and $\phi = 270°$ ($\theta_A = \theta_B = 90°$) and the A^+_1 and B^-_2 states correspond with the even and odd tunneling combinations. This degree of localization can be reached when the basis is converged, which it was found [11] to be with $j_A,j_B \leq 8$ for $ortho$-N_2 and $j_A,j_B \leq 9$ for $para$-N_2 (with five radial basis functions, $n \leq 4$); there is strong admixture between the different (even or odd) j_A,j_B values.

The results were compared with harmonic oscillator model results [11], in order to analyze the character of the vibrations in terms of normal modes. In the ground state the near-rigid harmonic oscillator limit is not too unrealistic (cf. the zero-point energy in Table III), although the librational amplitudes are not small (see Fig. 1). The first angularly excited states are still localised (cf. the B^+_1 state in Fig. 1, which is mainly the ϕ fundamental) and lying just below the tops of the effective internal rotation barriers, but they are strongly anharmonic already (cf. the fundamental frequencies in Table III) and penetrate into the classically forbidden regions around $\phi = 0°$ and $\phi = 180°$. In the higher excited states, such as the first excited A^+_1 state which corresponds with the ϕ overtone (Fig. 1), the monomers rotate almost freely. This free rotation does not occur in all directions simultaneously, however. For instance, in the first excited A^+_1 state only the torsional rotation (ϕ) about the binding axis R is free, while the bending (θ_A,θ_B) motions are still librations, localised around $\theta_A = \theta_B = 90°$. So, it is concluded [11] that the $(N_2)_2$ dimer displays both the features of a normal structured molecule, although rather floppy, in the ground state, and those of a system with nearly free internal rotations, at higher vibrational energies. In the
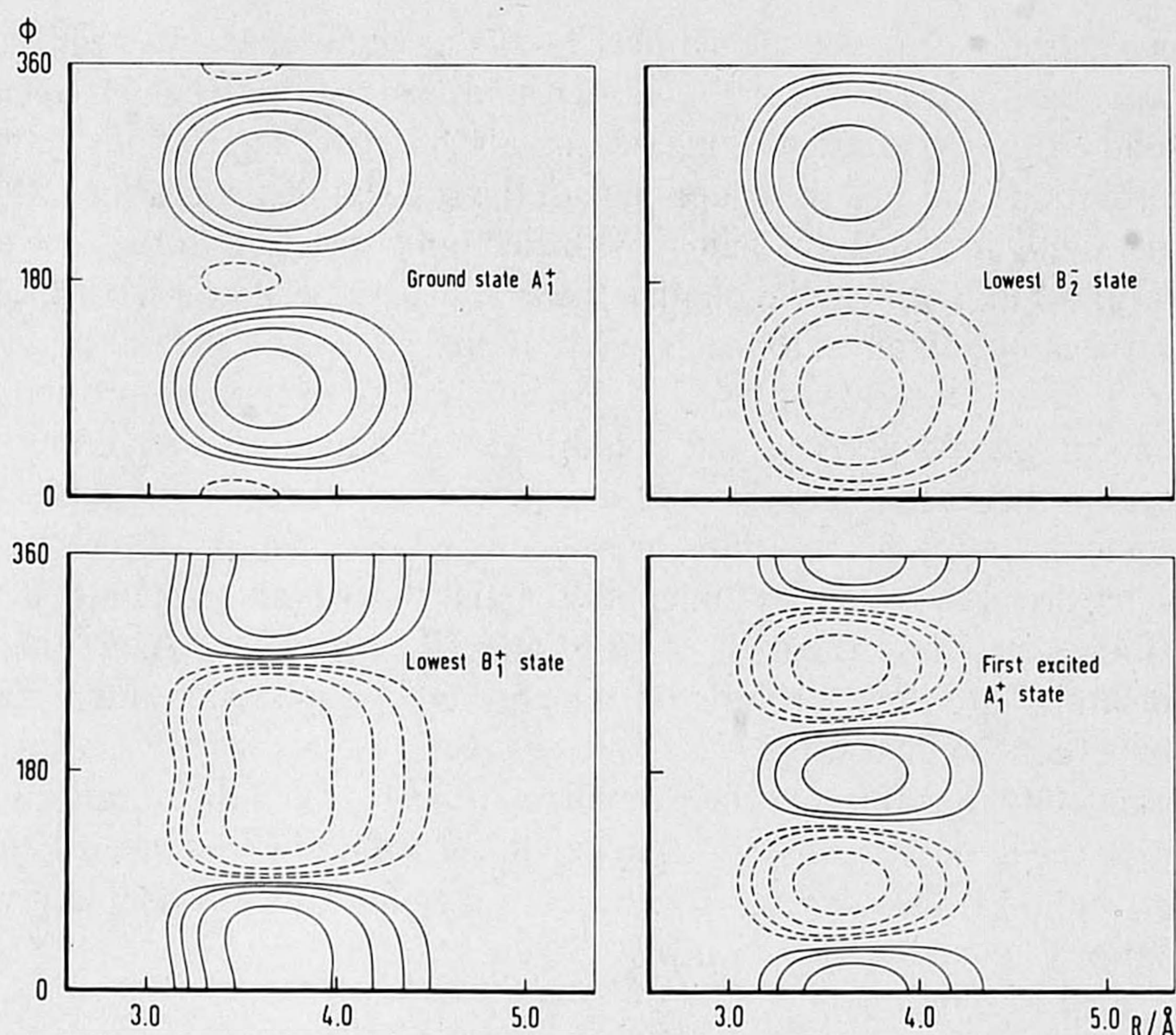
Figure 1. Cuts through the vibrational ($J = 0$) wave functions in $(N_2)_2$ for the lowest four states, with θ_A and θ_B fixed at 90°. The contours enclose regions with 8%, 16%, 32%, and 64% of the maximum amplitude. Solid curves correspond with positive values of the wavefunction and dashed curves with negative values.

intermediate range the internal rotations are free in specific directions. As a function of temperature one should be able to observe an orientational order–disorder transition, just as in the solid (but at lower temperatures, since the dimer is floppier than the solid, and without a sharp transition point).

The secular problem with basis (4) is analogous to the full configuration interaction

TABLE III.   Comparison of the fundamental vibration frequencies in $(N_2)_2$ from the harmonic oscillator model and from the full dynamical calculation [using Hamiltonian (3), with the *ab initio* potential (1), and the basis (4)] [11].

(Normal) coordinate	Symmetry		Energy (cm^{-1})	
	D_{2d}	$S_4' \otimes C_i$	Harmonic	Full
R	A_1	A_1^+	39.2	33.2
θ_A, θ_B	E	E^+	22.1	14.2
ϕ	B_1	B_1^+	13.9	8.1
zero-point energy			48.7	47.1

problem in electronic structure calculations. So the ro-vibrational states which emerge from this calculation are fully correlated (within the given finite basis). Speaking in terms of solid lattice dynamics, this means that all the (pair) correlations between the monomer librations and also the coupling with the translational vibrations (the dimer stretch) are exactly included. In analogy with electronic structure theory, one can look at the natural orbitals which diagonalize the first order density matrix [25,26]; this density matrix can be obtained for each ro-vibrational state from the full configuration interaction function in terms of basis (4) by integrating over the coordinates of all particles except one. As particles one could take the individual nuclei, but it seems more natural in this case where the centre of mass translational motion is separated off, the monomer stretch vibrations are decoupled and we are interested in the monomer librational motions, the dimer stretch and the overall rotation to define the following four "particles" (degrees of freedom): (θ_A, ϕ_A), (θ_B, ϕ_B), R, (β, α). The "natural orbitals" are those orbitals for which the "configuration interaction" expansion converges the fastest [25].

In order to study the effects of the pair correlations between the librations and the coupling with the dimer stretch vibration explicitly, we define the mean-field Hamiltonian for the librations (for $J = 0$, where we have no Coriolis coupling with the overall rotation)

$$H_A^{MF} = H_A + \langle \psi_B(\theta_B, \phi_B) | H_{AB} | \psi_B(\theta_B, \phi_B) \rangle, \tag{7}$$

where the "one-particle" term and the pair term are defined as

$$H_A = \frac{j_A^2}{2\mu_A r_A^2} + \left\langle \frac{1}{2\mu R^2} \right\rangle_R j_A^2, \tag{8}$$

$$H_{AB} = \langle V_{AB} \rangle_R + \left\langle \frac{1}{\mu R^2} \right\rangle_R \mathbf{j}_A \cdot \mathbf{j}_B, \tag{9}$$

and the mean-field wave functions ψ_B can be expanded as

$$\psi_B = \sum_{j_B, m_B} c_{j_B, m_B}^B Y_{j_B, m_B}(\theta_B, \phi_B). \tag{10}$$

Since these functions ψ_B must be the eigenvectors of the mean-field Hamiltonian H_B^{MF} which is analogous to Eq. (7) and contains the functions ψ_A, the problem has to be solved self-consistently. The expectation values over the dimer stretch coordinate R can be evaluated if this coordinate is also included in the mean-field procedure by defining an effective radial Hamiltonian (averaging the full Hamiltonian (3) over the angular wave functions $\psi_A \psi_B$). Alternatively, one can decouple the dimer stretch motion by solving the mean-field problem, Eqs. (7) to (10), for fixed distance R. Doing this for various R values, one obtains an effective radial potential in the Born–Oppenheimer sense, which can be used, then, to generate the radial solutions.

The latter way of decoupling the radial coordinate R from the angular problem by freezing it at various values, has just been performed [27], not for the mean-field problem but for full Hamiltonian (3). The results for $R = R_e = 3.46$ Å and $R = \langle R \rangle$ = 3.79 Å are shown in Figure 2, together with the results of the full radial and angular solution [11] of Hamiltonian (3). The comparison is quite interesting. At $R = R_e$, all the angular vibration frequencies are much too high and the order of the levels is
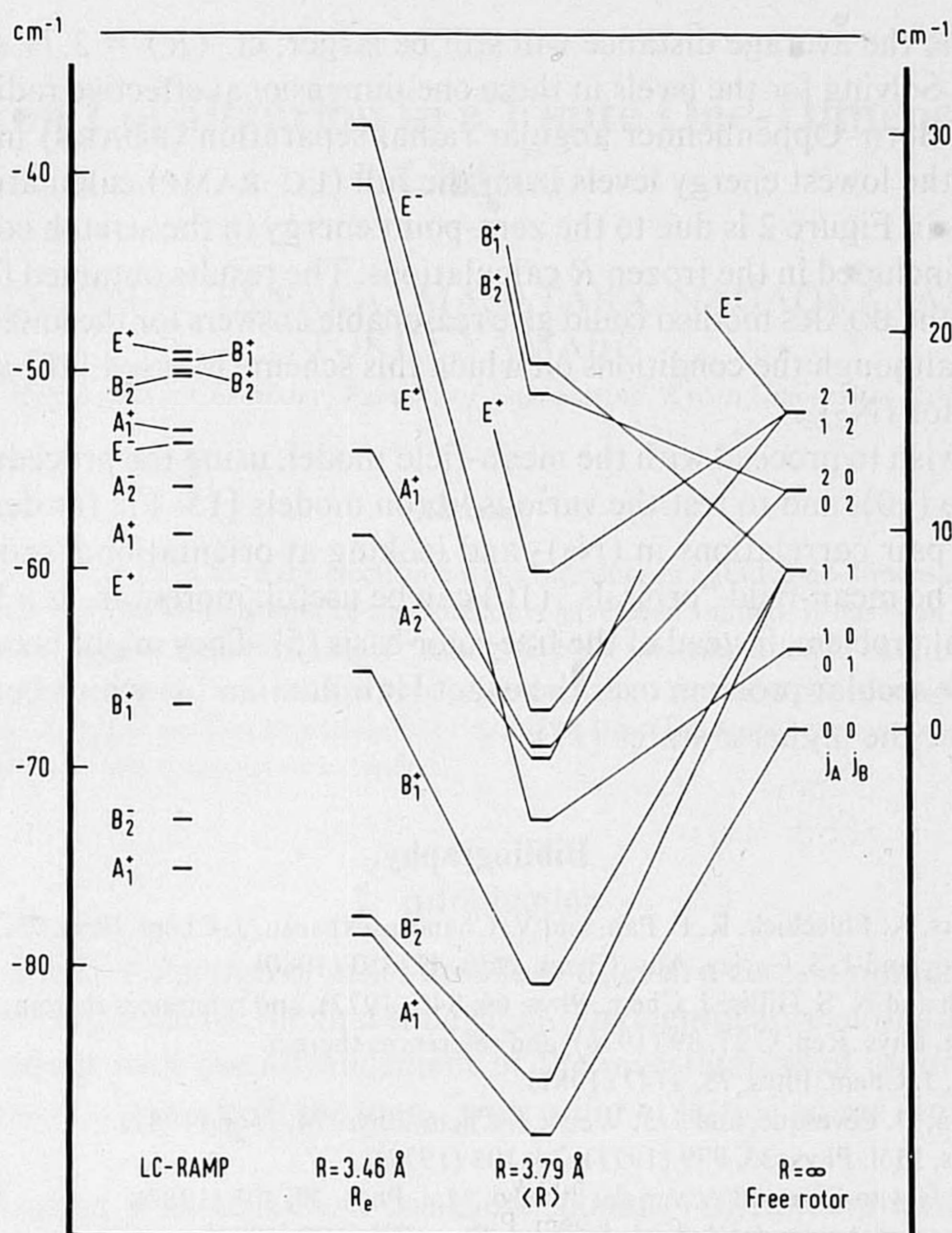
Figure 2. Vibrational ($J = 0$) energy levels in $(N_2)_2$ from the full dynamical [linear combination of radial and angular momentum products (LC–RAMP)] calculation [11], as compared with the angular vibrational levels calculated for fixed R (see text). The free rotor ($R = \infty$) levels are shifted (see right-hand energy scale) with respect to the others.

incorrect. At $R = \langle R \rangle$, the ground state average distance in the full calculation, the levels up to about 20 cm^{-1} above the ground state are quite well represented. These correspond with angular excitations [11]; apparently, the barriers to internal rotations felt by the monomers at $R = \langle R \rangle$ are similar to the effective barriers in the full calculation (whereas at $R = R_e$ they are much higher). Around 25 cm^{-1} above the ground state, the level ordering for $R = \langle R \rangle$ begins to deviate more strongly from the ordering in the full calculation. This is due to the interaction (Fermi resonance) between the angular overtones and the first dimer stretch excitation at 33 cm^{-1}. We conclude that freezing R at $\langle R \rangle$ (which might be the experimental ground state average distance) yields reasonable values for the fundamental libration frequencies, as well as for the tunneling frequency.

The energy levels calculated [27] for a range of (frozen) distances R form a set of potential curves for the radial problem. For the ground state the minimum in the curve lies at $R = 3.65$ Å, which is substantially larger than $R_e = 3.46$ Å. (Since the curve

is asymmetric the average distance will still be larger; cf. $\langle R \rangle = 3.79$ Å in the full calculation.) Solving for the levels in these one-dimensional effective radial problems is called the Born–Oppenheimer angular radial separation (BOARS) method [28]. The shift in the lowest energy levels from the full (LC–RAMP) calculation to the $R = \langle R \rangle$ levels in Figure 2 is due to the zero-point energy in the stretch coordinate R, which is not included in the frozen R calculations. The results obtained for $R = \langle R \rangle$ indicate that the BOARS method could give reasonable answers for the lowest excitation frequencies, although the conditions on which this scheme is based [28] are certainly not fulfilled for $(N_2)_2$.

Next, we wish to proceed with the mean-field model, using the procedure outlined in Eqs. (7) to (10), and to test the various libron models [15–17] for describing the effect of the pair correlations in $(N_2)_2$ and looking at orientational order–disorder transitions. The mean-field "orbitals" (10) can be useful, moreover, as a basis for the full dynamical problem, instead of the free rotor basis (5). They might help in reducing the size of the secular problem over the exact Hamiltonian (3) which becomes quite formidable for the higher J states [11].

Bibliography

[1] R. D. Etters, K. Flurchick, R. P. Pan, and V. Chandrasekharan, J. Chem. Phys. **75**, 929 (1981).
[2] R. J. Le Roy and J. S. Carley, Adv. Chem. Phys. **42**, 353 (1980).
[3] J. C. Raich and N. S. Gillis, J. Chem. Phys. **66**, 846 (1977), and references therein.
[4] T. A. Scott, Phys. Rep. C **27**, 89 (1976), and references therein.
[5] G. Fiorese, J. Chem. Phys. **75**, 4747 (1981).
[6] M. L. Klein, D. Lévesque, and J. J. Weiss, J. Chem. Phys. **74**, 2566 (1981).
[7] D. J. Evans, Mol. Phys. **33**, 979 (1977); **34**, 103 (1977).
[8] F. Mulder, G. van Dijk and A. van der Avoird, Mol. Phys. **39**, 407 (1980).
[9] R. M. Berns and A. van der Avoird, J. Chem. Phys. **72**, 6107 (1980).
[10] T. Luty, A. van der Avoird, and R. M. Berns, J. Chem. Phys. **73**, 5305 (1980).
[11] J. Tennyson and A. van der Avoird, J. Chem. Phys. **77**, 5664 (1982).
[12] S. Califano, V. Schettino, and N. Neto, *Lattice Dynamics of Molecular Crystals*, Lecture Notes in Chemistry, Vol. 26 (Springer, Berlin, 1981).
[13] N. R. Werthamer, in *Rare Gas Solids*, M. L. Klein and J. A. Venables, Eds. (Academic, London, 1976), Vol. I, p. 265.
[14] T. Wasiutynski, Phys. Status Solidi B **76**, 175 (1976).
[15] J. C. Raich, J. Chem. Phys. **56**, 2395 (1972).
[16] P. V. Dunmore, J. Chem. Phys. **57**, 3348 (1972); Can J. Phys. **55**, 554 (1977).
[17] M. J. Mandell, J. Low. Temp. Phys. **17**, 169 (1974); **18**, 273 (1975).
[18] D. M. Brink and G. T. Satchler, *Angular Momentum*, 2nd Ed. (Clarendon, Oxford, 1968).
[19] W. Briels and A. van der Avoird (unpublished).
[20] J. Verberne and J. Reuss, Chem. Phys. **50**, 137 (1980); **54**, 189 (1981).
[21] M. Waaijer, M. Jacobs, and J. Reuss, Chem. Phys. **63**, 257 (1981).
[22] T. R. Dyke, B. J. Howard, and W. Klemperer, J. Chem. Phys. **56**, 2442 (1972).
[23] J. Tennyson and B. T. Sutcliffe, J. Chem. Phys. **77**, 4061 (1982).
[24] P. M. Morse, Physica (Utrecht) **34**, 57 (1929).
[25] P.-O. Löwdin, Phys. Rev. **97**, 1474 (1955); **97**, 1490 (1955); **97**, 1509 (1955); Adv. Chem. Phys. **2**, 207 (1959).
[26] A. C. Hurley, *Electron Correlation in Small Molecules* (Academic, London, 1976).
[27] M. Claessens and Th. van der Lee, Internal Report, Institute of Theoretical Chemistry, Nijmegen (1982).
[28] S. L. Holmgren, M. Waldman, and W. Klemperer, J. Chem. Phys. **67**, 4414 (1977).